

Synthesis, Electrochemical Characterization of $\text{Al}_2\text{O}_3\text{-CeO}_2$ Mixed Oxide Nano Particles

R. R. Muthuchudarkodi¹, S. Kalaiarasi²

¹Department of Chemistry, V. O. Chidambaram College, Thoothukudi-628008, India

²Department of Chemistry A. P. C. Mahalaxmi College Thoothukudi-628008, Tamilnadu, India

Abstract: Nano $\text{Al}_2\text{O}_3\text{-CeO}_2$ mixed oxides were prepared by wet chemical method by mixing equimolar solutions of Aluminiumsulphate(0.1M) and Cerium nitrate(0.1M) in aqueous Sodium hydroxide and refluxed at elevated temperature. The prepared nano $\text{Al}_2\text{O}_3\text{-CeO}_2$ mixed oxides were characterized by UV-Vis, XRD, TEM and CV studies. From UV –Visible spectra of $\text{Al}_2\text{O}_3\text{-CeO}_2$ mixed metal oxide nano particles exhibited absorption at 302 nm and 348 nm. The blue shifted absorption peaks of simple and mixed metal oxide nano particles showed nano scale effect. From XRD studies the size of the nano $\text{Al}_2\text{O}_3\text{-CeO}_2$ was found to be 1.7nm through Debye-Scherrer's formula. The size of synthesized nano particles were further confirmed by TEM and it was found to be 50nm. Cyclic Voltammetric studies exhibit good adherent behaviour on electrode surface and good electroactivity at pH 1.0.

Keywords: $\text{Al}_2\text{O}_3\text{-CeO}_2$, UV-Visible spectra, Cyclic Voltammetry, TEM

1. Introduction

Metal oxides play a very important role in many areas of chemistry, physics and materials science [1]. The metal elements are able to form a large diversity of oxide compounds [2]. These can adopt a vast number of structural geometries with an electronic structure that can exhibit metallic, semiconductor or insulator character. In technological applications, oxides are used in the fabrication of microelectronic circuits, sensors, piezoelectric devices, fuel cells, coatings for the passivation of surfaces against corrosion, and as catalysts. In the emerging field of nanotechnology, a goal is to make nano structures or nano arrays with special properties with respect to those of bulk or single particle species [3].

Ceria (CeO_2) is an important rare-earth oxide that has been attracting a-growing attention because of its varied applications in fuel cells,[4]-[8] oxygen gas sensors,[9]polishing agents,[10] oxygen permeation membrane systems,[11][12] and as catalysts for different technologically important processes.[13]-[18] Ceria is an essential component of the three-way catalyst (TWC), which is being used for environment cleaning purposes, as well as different emerging fields of catalysis such as oxidation of hydrocarbons,[19] removal of total organic carbon from waste,[20] automobile exhaust gas conversion [21][22]. The possibility of transformation from Ce^{3+} and Ce^{4+} aids in accepting or removing oxygen from ceria. In addition, the fluorite structure of ceria or doped ceria has superior chemical and physical stability [23]. Pure CeO_2 alone as a catalyst is probably of little interest because of its low textural stability under high-temperature conditions, usually encountered in exhaust gases. At high temperatures, not only does the surface area of CeO_2 reduce drastically, but it also loses its redox properties and oxygen storage capacity [24]. It has been observed that ceria with suitable dopants (specially rare-earth oxide) improves its stability toward sintering and the catalytic activity of the resulting catalysts [25]. The versatility of rare-earth doped ceria depends on availability of the 4f shell. On substitution of the trivalent

rare-earth element, the oxygen vacancies increase; this in turn improves oxygen mobility and oxygen storage capacity [26].

Corrosion resistance can be excellent due to a thin surface layer of aluminium oxide that forms when the metal is exposed to air, effectively preventing further oxidation. The strongest aluminium alloys are less corrosion resistant due to galvanic reactions with alloyed copper[27].This corrosion resistance is also often greatly reduced by aqueous salts, particularly in the presence of dissimilar metals[28].

2. Experimental Methods

2.1 Preparation of CeO_2 nano metal oxides

Ceria nanoparticles were synthesized by using cerium nitrate and sodium hydroxide as precursors. All the reagents were of analytical grade and used without further purification. The entire process was carried out in deionised water for its inherent advantages of being simple and environment friendly. In a typical preparation, solution of 0.1M cerium nitrate was prepared in 50ml of deionised water and then 50ml of aqueous solution of 2M Sodium hydroxide was added dropwise to this solution making a final volume of 100ml. This mixture was stirred well and refluxed for 3hr at a temperature of about 80°C which resulted in the formation of light yellow ceria nano particles. The precipitate was separated from the reaction mixture, washed several times with deionised water to remove the impurities. The precipitate was dried at room temperature. Similar procedure was carried out for the preparation of Al_2O_3 nanoparticles using $\text{Al}_2(\text{SO}_4)_3$ as precursor.

2.2 Preparation of $\text{Al}_2\text{O}_3\text{-CeO}_2$ mixed oxide nanoparticles

$\text{Al}_2\text{O}_3\text{-CeO}_2$ mixed oxide nanoparticles were prepared at room temperature by wet chemical method. 50 ml of 0.1M solution of Cerium nitrate and 50ml of 0.1M solution of Aluminiumsulphate solutions were mixed. 100 ml of 2M

Sodium hydroxide solution was added drop wise to the above mixture. The resulting solution was refluxed for 3hr at a temperature of 80°C. The white precipitate was obtained. The obtained precipitate was filtered and the filtrate was washed several times with deionised water to remove the impurities. The precipitate was dried at room temperature. Similar procedure was repeated for the preparation of different concentrations of mixed metal oxide nanoparticles by varying the concentrations of both $Al_2(SO_4)_3$ and Cerium nitrate in the range of 0.05-0.2M.

3. Characterization

Computer controlled JASCO V-530 was used to study UV-VIS spectral behaviour. The X-ray diffraction (XRD) patterns were recorded for the powdered materials using a BRUKER AXS (D8 ADVANCE) X-ray diffractometer. TEM images were recorded using Philips CM 200 model with the operating voltage range of 20-200 and with a resolution of 2.4 \AA . Cyclic Voltammetric studies were carried out using electrochemical workstation (mode 650C), CH-Instrument.

4. Result and Discussion

4.1 UV-Visible Studies

Optical properties of the CeO_2 nanoparticles samples were studied by UV-Vis spectrum. It can be seen from the Fig.1 that there is an intensive absorption in the ultraviolet band of about 200-800nm. The absorption wavelength appears at about 292nm for CeO_2 nanoparticles [29]. UV-Visible spectra of Al_2O_3 nanoparticles is shown in Fig.2. The absorption peak for Al_2O_3 nanoparticles has been found to be at 342nm.

UV-visible absorption spectra of the $Al_2O_3-CeO_2$ mixed oxide is recorded in the wavelength range of 200-800nm. Fig.3 represents the UV-visible absorption spectrum of the $Al_2O_3-CeO_2$ mixed oxide. The absorption peak for nano $Al_2O_3-CeO_2$ mixed oxide has been found to be at 302nm.

The variation in the absorption peaks for simple and mixed oxide nanoparticles are due to the smaller size of nanoparticles [30]. The mixed oxide nanoparticles exhibited more than 40nm blue shift compared with that of the simple oxide nanoparticles. The blue shift of the absorption peaks of metal oxide nanoparticles result from certain unique effects of nano materials such as nano scale effect and the blue shift reduce absorption of UV rays of longer wave length and is thus undesirable for UV protection. The absorption peaks of mixed oxide appeared at shorter wavelength region and are thus used as a solar UV blockers [31].

4.2 UV-Visible Spectrum

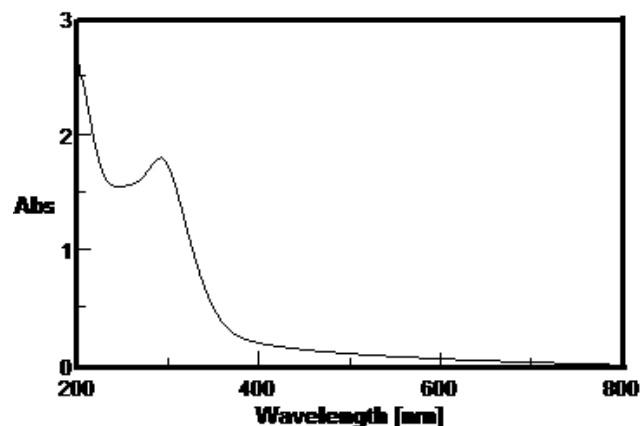


Figure 1: UV-VIS Spectrum of CeO_2 nanoparticles

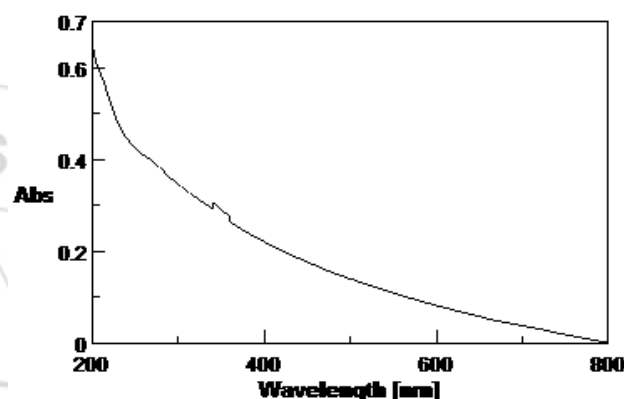


Figure 2: UV-VIS Spectrum of Al_2O_3 nanoparticles

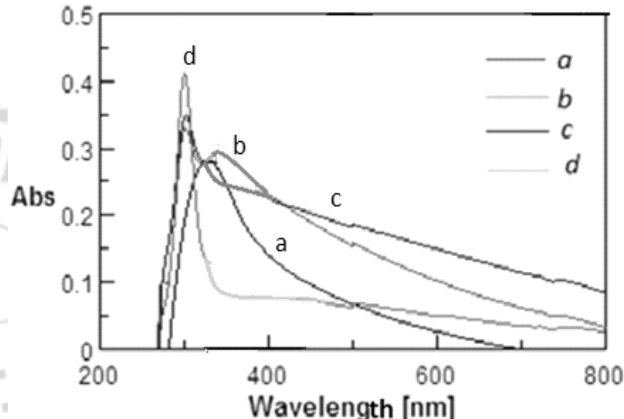


Figure 3: UV-VIS Spectra of a) 0.05M $Al_2O_3-CeO_2$ b) 0.1M $Al_2O_3-CeO_2$ c) 0.15M $Al_2O_3-CeO_2$ d) 0.2M $Al_2O_3-CeO_2$ mixed oxide nanoparticles

4.3 XRD

Structural properties of the prepared metal oxide nanoparticles were studied by X-Ray Diffraction analysis. The crystallite size was calculated by using the Debye-Scherer formula as given in equation (1)

$$D = k\lambda / \beta \cos\theta \quad \text{-----(1)}$$

Where λ is the wavelength of radiation used (1.54060 \AA for Cu K radiation), k is the Scherrer constant equal to 0.94, β is the full width at half maximum (FWHM) intensity of the diffraction peak for which the particle size is to be calculated, θ is the diffraction angle of the concerned diffraction peak and D is the crystalline size in nanometers (nm).

The XRD pattern of the CeO₂ nanoparticles is shown in the (Fig.4). It shows three diffraction peaks at 2θ values of 28.5950, 33.1164, and 47.5123. The values of (β) observed for ceria is 0.5353, 0.6691, and 0.7360. The peaks are identified to originate from (111), (200), and (220) planes of the cubic phase of Ceria respectively [32]. Based on the Scherrer's equation, the average crystallite size of the nanoparticles is calculated as 28nm. This spectrum was well matched with the standard (JCPDS 01-075-0390).

The XRD pattern of nano Al₂O₃-CeO₂ mixed oxide nanoparticles are shown in (Fig:5).The main diffraction peaks are observed at 2θ values of 16.1333, 29.3890, 31.3456, and 48.6077. The values of (β) observed for Al₂O₃-CeO₂ mixed oxides are 0.0836,0.1004, 0.1004 and 0.1020. All detectable peaks were identified to originate from (211), (411),(421), and (632) planes. Based on the Scherrer's equation, the average crystallite sizes of the nanoparticles are observed to be 1.7nm.

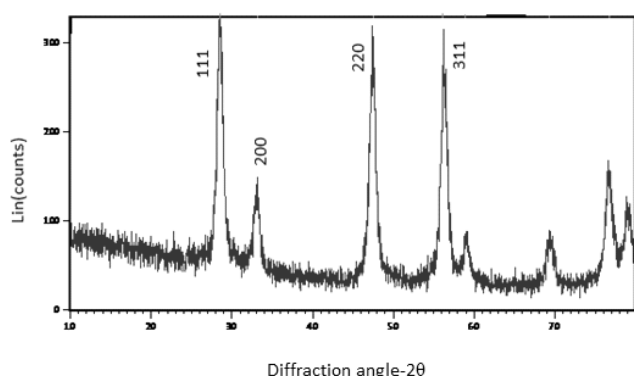


Figure 4: XRD pattern of nano CeO₂ mixed oxide

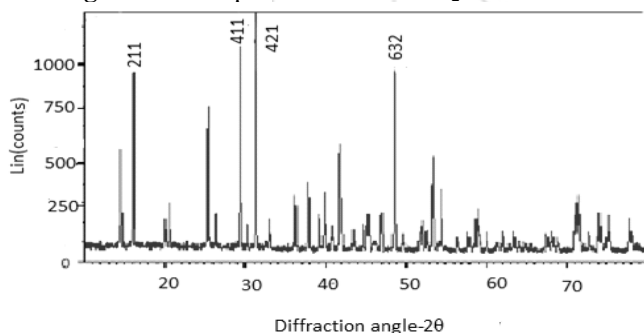


Figure 5: XRD pattern of nano Al₂O₃- CeO₂ mixed oxide

4.4 TEM

The size of synthesized nanoparticles was further confirmed by TEM. The Transmission Electron Microscopy (TEM) image of Al₂O₃-CeO₂ mixed oxides are shown in (Figs.6).The size of Al₂O₃-CeO₂ mixed oxide is found to be 50 nm (Fig.6). Electron diffraction of the selected area of nano Al₂O₃-CeO₂ mixed oxide showed two circular rings and are shown in (Fig :7).The pattern display distinct as opposed to being the powder pattern type confirm that the crystal growth is epitaxial with respect to the monolayer and demonstrate that this lattice correspondence is maintained even in regions of denser crystal coverage .The appearance of some darker particles diffraction contrast due to their orientation with mixed oxide is shown in (Fig:7) which revealed that the samples are semi crystalline (211),(411),(422) and (632) phase.

From the results obtained it has been demonstrated that the size of nano Al₂O₃-CeO₂ mixed oxides are in the range of 50 nm. The Selected Area Electron Diffraction pattern exhibiting several uniform bright rings suggested that the nanocrystals are semi crystalline.

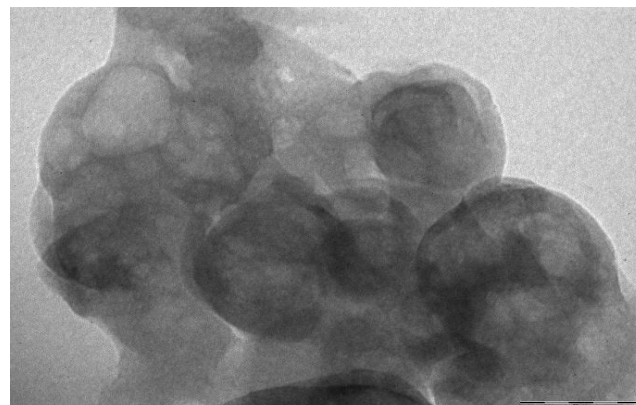


Figure 6: TEM image of nano Al₂O₃-CeO₂ mixed oxide

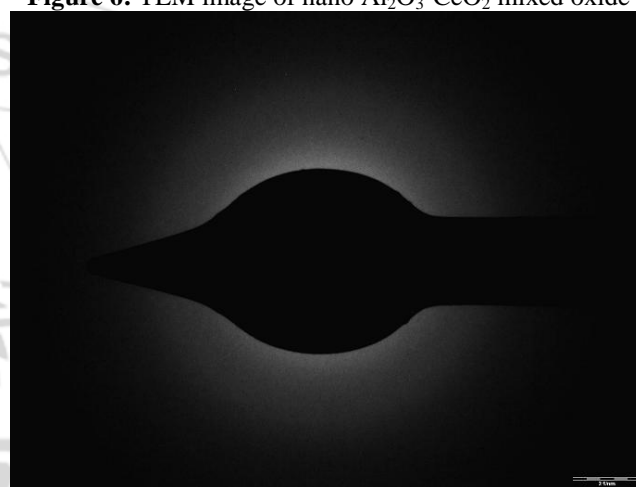


Figure 7: SAED pattern of nano Al₂O₃-CeO₂ mixed oxide

4.5 Cyclic Voltammetry

Cyclic voltammetric behaviour of the nano mixed oxides is recorded using electrochemical workstation. The potential window is between -0.6 to 1.4V on GCE at 50mv/s. Cyclic voltammetric behavior of CeO₂ showed one oxidation peak (Fig.8) at -0.1175V which is due to the presence of CeO₂. Cyclic voltammetric behaviour of nano Al₂O₃-CeO₂(0.1M) mixed oxide showed one oxidation peak (Fig.9) at -0.1995 which is entirely different from the behavior of CeO₂ confirms the formation of Al₂O₃-CeO₂ mixed oxides.

Cyclic voltammetric behaviour of Al₂O₃-CeO₂ mixed oxides at different scan rates are shown in (Fig.10).The plot of peak current versus scan rate for nano Al₂O₃-CeO₂mixed oxides (Fig.11) gave a straight line indicating a good adherent behavior on electrode surface. Thus the mixed oxides act as corrosive resistance agents. Peak currents of nano Al₂O₃-CeO₂ are correlated with the square root of scan rate (Fig.12), a straight line is observed. These facts revealed that the voltammetric redox behavior of mixed metal oxide nanoparticles is controlled by adsorption process.

5. Cyclic Voltammogram

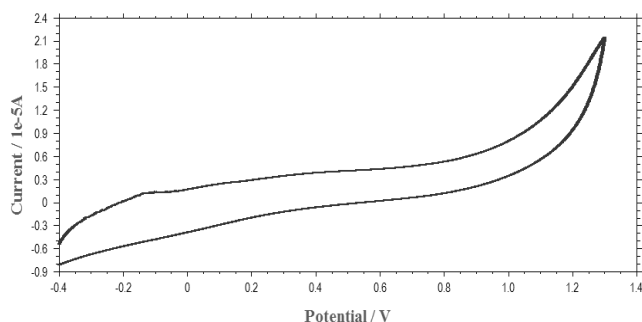


Figure 8: Cyclic Voltammogram of CeO₂ nanoparticles

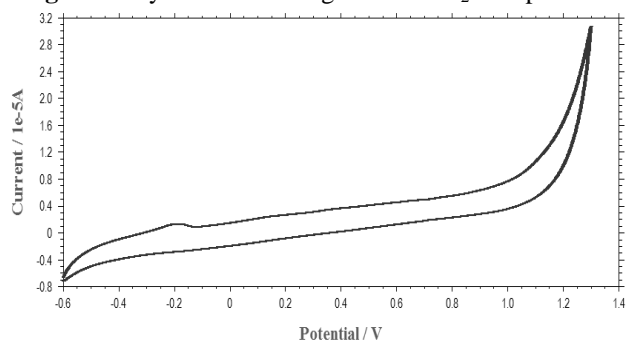


Figure 9: Cyclic Voltammogram of nano Al₂O₃-CeO₂ mixed oxide

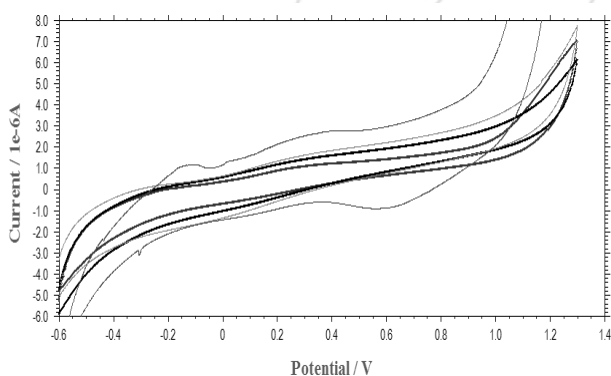


Figure 10: Cyclic voltammetric behaviour of nano Al₂O₃-CeO₂ mixed oxides at different scan rates 15, 25, 35 and 45 mVs⁻¹

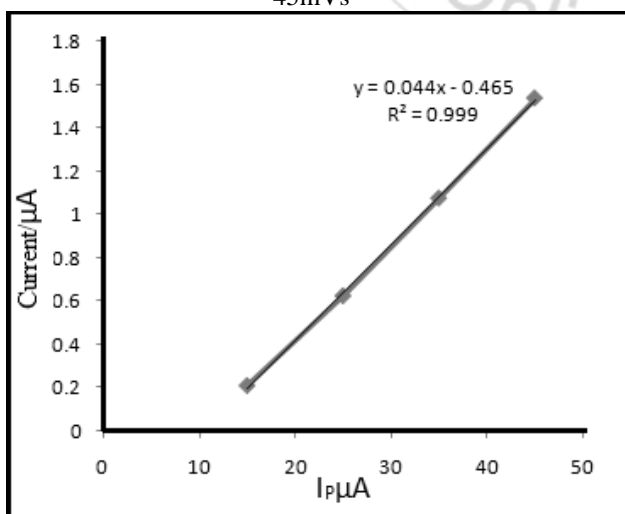


Figure 11: Plot of peak current versus scan rate for nano Al₂O₃-CeO₂ mixed oxide

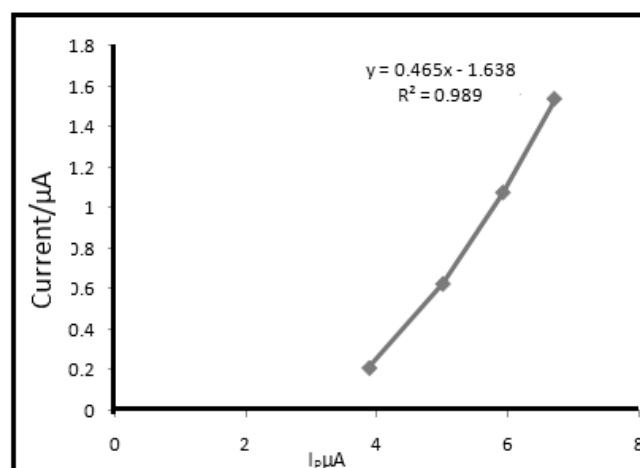


Figure 12: Plot of peak current versus square root of scan rate for nano Al₂O₃-CeO₂ mixed oxide nanoparticles

6. Conclusion

Nano Al₂O₃-CeO₂ and MoO₃-CeO₂ mixed oxides are synthesized by wet chemical method. The mixed metal oxide nanoparticles are characterized by UV, XRD, TEM and Cyclic Voltammetry. The blue shifted absorption peaks of simple and mixed metal oxide nanoparticles showed nano scale effect. XRD behavior also suggested the mixed oxide nanoparticles are in the nano scale range. The surface morphology of the synthesized mixed oxide nanoparticles exhibited different structures. TEM images also confirmed the particle size of the mixed oxide nanoparticles in the nano scale range. From cyclic voltammetric studies the mixed metal oxide nanoparticles exhibited good adherent behaviour on electrode surface and are adsorption controlled and revealed good electroactivity.

From this investigation the synthesized mixed metal oxide nanoparticles have been observed as corrosive resistant. Thus the mixed oxides can be used as a potential, electrode material and for further electronic applications.

7. Acknowledgement

The authors are extremely grateful to Department of Science and Technology (FAST TRACK and FIST) New Delhi, Jasco UV-VISIBLE Spectrophotometer and CH Electrochemical Workkstation at V.O.C.College, Tuticorin-8.

References

- [1] C.Noguera, *Physics and Chemistry at Oxide Surfaces*; Cambridge University Press:Cambridge, UK, (1996).
- [2] R.W.G.Wyckoff, *Crystal Structures, 2nd ed*; Wiley: New York, (1964).
- [3] H.Gleiter, *Nanostruct. Mater.*6, (1995) 3.
- [4] S.J. Park, J.M. Vohs, and R.J. Gorte: Direct oxidation of hydrocarbons in a solid-oxide fuel cell. *Nature* 265, ((2000) 404..
- [5] E.P. Murray, T. Tsai, and A. Barnett: A direct-methane fuel cell with a ceria-based anode. *Nature* 400, (1999) 649.
- [6] Y. Maki, M. Matsuda, and T. Kudo: U.S. Patent No. 3 [607],(1971) 424.

- [7] V.V. Kharton, F.M. Figueiredo, L. Navarro, E.N. Naumovich, A.V. Kovalevsky, A.A. Yaremchenko, A.P. Viskup, A. Carneiro, F.M.B. Marques, and J.R. Frade: Ceria-based materials for solid oxide fuel cells. *J. Mater. Sci.* 36, (2001) 1105.
- [8] A.I.Y. Tok, L.H. Luo, F.Y.C. Boey, and S.H. Ng: Consolidation and properties of Gd_{0.1}Ce_{0.9}O_{1.95} nanoparticles for solid oxide fuel cell electrolytes. *J. Mater. Res.* 21, (2006) 19.
- [9] N. Izu, W. Shin, and N. Murayama: Fast response of resistive type oxygen gas sensors based on nano-sized ceria powder. *Sens. Actuators, B* 93, (2003) 449.
- [10] N.B. Kirk and J.V. Wood: Glass polishing. *Br. Ceram. Trans.* 93, (1994) 25.
- [11] X. Yin, L. Hong, and Z-L. Liu: Development of oxygen transport membrane La_{0.2}Sr_{0.8}CoO_{3-d}/Ce_{0.8}Gd_{0.2}O_{2-d} on the tubular CeO₂ support. *Appl. Catal., A* 300, (2006) 75.
- [12] X. Yin, L. Hong, and Z-L. Liu: Oxygen permeation through the LSCO-80/CeO₂ asymmetric tubular membrane reactor. *J. Membr. Sci.* 268, (2006) 2.
- [13] S. Damayanova and J.M.C. Bueno: Effect of CeO₂ loading on the surface and catalytic behaviors of CeO₂-Al₂O₃-supported Pt catalysts. *Appl. A. Catal.*, 253, (2003) 135.
- [14] Y.F. Yao and J.T. Kummer: Low-concentration supported precious metal catalysts prepared by thermal transport. *J. Catal.* 106, (1987) 307.
- [15] E.C. Su, C.N. Montreuil, and W.G. Rothschild: Oxygen storage capacity of monolith three-way catalysts. *Appl. Catal.* 17, (1985) 75.
- [16] S. Imamura, I. Fukuda, and S. Ishida: Wet oxidation catalyzed by ruthenium supported on cerium (IV) oxides. *Ind. Eng. Chem. Res.* 27 (1988) 718.
- [17] V.S. Mishra, V.V. Mahajani, and J.B. Joshi: Wet air oxidation. *Ind. Eng. Chem. Res.* 34, (1995) 2.
- [18] A. Trovarelli, C. de Leitenburg, M. Boaro, and G. Dolcetti: Redox chemistry over CeO₂-based catalysts: SO₂ reduction by CO or CH₄. *Catal. Today* 50, (1999) 381.
- [19] S. Zhao and R.K. Gorte: A comparison of ceria and Sm-doped ceria for hydrocarbon oxidation reactions. *Appl. Catal., A* 277, (2004) 129.
- [20] S. Kawi, Y.P. Tang, K. Hidajat, and L.E. Yu: Synthesis and characterization of nanoscale CeO₂ catalyst for deNO_x. *J. Metastable Nanocryst. Mater.* 23, (2005) 95.
- [21] M.K. Neylon, M.J. Castagonla, N.B. Castagonla, and C.L. Marshall: Coated bifunctional catalysts for NO_x SCR with C₃H₆: Part I: Water-enhanced activity. *Catal. Today* 96, (2004) 53.
- [22] G. Colon, J.A. Navio, R. Monaci, and I. Ferino: CeO₂-La₂O₃ catalytic system Part I. Preparation and characterisation of catalysts. *Phys. Chem. Chem. Phys.* 2, (2000) 4453.
- [23] K. Krishna, A. Bueno-Lopez, M. Makkee, and J.A. Moulijn: Potential rare earth modified CeO₂ catalysts for soot oxidation. I. Characterisation and catalytic activity with O₂. *Appl. B. Catal.* 75, (2007) 189.
- [24] U. Hennings and R. Reimert: Noble metal catalysts supported on gadolinium doped ceria used for natural gas reforming in fuel-cell applications. *Appl. Catal. B* 70, (2007) 498.
- [25] F.X. Liu, C.Y. Wang, Q.D. Su, T.P. Zhao, and G.W. Zhao: Optical properties of nanocrystalline ceria. *Appl. Opt.* 36, (1992) 7967.
- [26] Deshpande, Sameer; Patil, Swanand; Kuchibhatla, Satyanarayana VNT; Seal, Sudipta. "Size dependency variation in lattice parameter and valency states in nanocrystalline cerium oxide". *Applied Physics Letters* 87 (13) : (2005) 133113.
- [27] H. A. Macleod, *Thin-film optical filter* CRC Press. pp. 158-159. (2001) ISBN0-7503-0688-2.
- [28] L. E. Hetherington, *World Mineral Production: 2001-2005*. British Geological Survey. (2007) ISBN978-0-85272-592-4.
- [29] BS Rema Devi, R. Raveendren and Av Vaidyan. *Pramana - J. Physics* Vol.68, No.4, April (2007) 679-687.
- [30] F. Zhang, *et al.*, *Appl. Phys. Lett.* 80, (2002) 127.
- [31] D K Singh, D K Pandey, R R Yadav and Devaraj Singh *Pramana - J. Phys.*, Vol.78, No.5, May (2012) 759-766.
- [32] E. G. Heckert, A. S. Karakoti, S. Seal, and W. T. Self, The role of cerium redox state in the SOD mimetic activity of Nanoceria. *Biomaterials* 29, (2008) 2705.